INORGANIC CHEMISTRY FRONTIERS

RESEARCH ARTICLE

View Article Online
View Journal | View Issue

Cite this: *Inorg. Chem. Front.*, 2022, **9**, 1134

Porosity regulation of metal–organic frameworks for high proton conductivity by rational ligand design: mono- *versus* disulfonyl-4,4′-biphenyldicarboxylic acid†

Shunlin Zhang,[a] Yuxin Xie,[a] Mengrui Yang[a] and Dunru Zhu *[a,b]

Received 24th December 2021,
Accepted 28th January 2022

DOI: 10.1039/d1qi01610e

rsc.li/frontiers-inorganic

Porous crystalline metal–organic frameworks (MOFs) bearing sulfonic groups (–SO_3H) are receiving increasing attention as solid-state proton conductors because the –SO_3H group can not only enhance the proton concentration, but also form hydrogen bonding networks for high proton conductivity. A large number of 1,4-phenyldicarboxylic acids or biphenyldicarboxylic acids bearing two –SO_3H groups have been applied for the synthesis of proton-conducting MOFs. Surprisingly, 4,4′-biphenyldicarboxylic acid bearing one –SO_3H group has never been explored for the construction of proton-conducting materials. Herein, we first designed and synthesized 2-sulfonyl-4,4′-biphenyldicarboxylic acid (H_3L). By applying this ligand to react with lanthanide salts, a series of three-dimensional MOFs, $(Me_2NH_2)_2(H_3O)[LnL_2]\cdot 8H_2O$ (Ln = Eu (**1**), Gd (**2**), Tb (**3**)) have been prepared. Due to the presence of the uncoordinated –SO_3H group and the encapsulation of high concentrations of dimethylammonium and hydronium cations in the cavity, the MOFs **1–3** show a high proton conductivity (8.83×10^{-3} S cm^{-1}) at 95 °C and 60% relative humidity (RH). More importantly, this high proton conductivity can be maintained over 72 hours without any significant decrease at low RH.

1. Introduction

Solid-state proton conductors (SSPCs) as important components of fuel cells, electrochemical sensors and reactors are attracting great interest.[1,2] Compared with traditional materials such as Nafion, porous crystalline MOF materials are considered to be one of the most promising next generation conductors as the crystal structures can be finely tuned by judicious selection of metal ions, ligands and appropriate post-synthesis modifications.[3,4] During the past few decades, significant progress in proton conductive MOFs has been achieved with the conductivity already exceeding 10^{-2} S cm^{-1}.[5–7] However, to maintain the conductivity at these high levels, the conductors must remain in a high relative humidity (RH) environment (>90% RH), which poses significant challenges, including the energy expenditure associated with maintaining the high humidity and the loss of fuel cell performance due to the possible flooding of the cathode.[8,9] Therefore, the development of novel SSPCs that maintain high proton conductivity at low RH is an urgent issue. There are usually two representative solutions: the first approach is to introduce small protic molecules into the cavity of MOFs, such as phosphonic acids,[10,11] imidazoles[12] and ionic liquids[13–15] and the second approach involves the functionalization of ligands with hydrophilic groups for an enhanced binding ability of the resulting MOFs to water molecules.[16,17]

Sulfonated species are highly hydrophilic and those bearing free –SO_3H groups are strong acids with a relatively low pK_a value (generally less than 0).[18] Consequently, sulfonated materials can interact with water molecules forming proton clusters in the form of $-SO_3^-\cdots H_3O^+$ and significantly increase the proton conductivity in a low RH environment.[19] Several methods for anchoring the acidic sulfonic groups to MOF pores have been developed including sulfonation of MOFs *via* post-synthesis,[20–22] sulfonation of organic linkers,[23] and coordination of sulfonic acid to metal centres.[24,25] Unfortunately, the modified MOFs are seldom examined by single crystal X-ray diffraction analysis; as a result, an in depth understanding of the precise H-bonding networks and proton conducting pathway is difficult. Sulfonic group substituted

[a]*College of Chemical Engineering, State Key Laboratory of Materials-oriented Chemical Engineering, Nanjing Tech University, 30 Puzhu South Road, Nanjing, Jiangsu 211816, China. E-mail: zhudr@njtech.edu.cn*
[b]*State Key Laboratory of Coordination Chemistry, Nanjing University, 163 Xianlin Avenue, Nanjing, Jiangsu 210023, China*

†Electronic supplementary information (ESI) available: FT-IR and ^{1}H NMR spectra of H_3L, the molecular structures, FT-IR spectra, PXRD patterns, and TGA curves of **1–3**, and the proton conductivity measurement of **2**. CCDC 2054977–2054979 for **1–3**. For ESI and crystallographic data in CIF or other electronic format see DOI: 10.1039/d1qi01610e

carboxylic ligands can be regarded as appealing candidates for the construction of proton conductive MOFs and some MOFs have also been characterized by single crystal X-ray diffraction analysis.[19,26] Commonly used ligands for the preparation of proton conductive MOFs include dipotassium-3,3′-disulfonyl-4,4′-biphenyldicarboxylic acid (3,3′-**DSBPDC**),[27] 3,3′-disulfonyl-benzophenone-4,4′-dicarboxylic acid (**DSBODC**),[28] 3,3′-disulfonyl-diphenylsulfone-4,4′-dicarboxylic acid (**DSDPSDC**),[29] disodium 2,2′-disulfonate-4,4′-oxydibenzoic acid (**DSOA**),[30–32] and 2,2′-disulfonyl-4,4′-biphenyldicarboxylic acid (2,2′-**DSBPDC**).[33,34] All these ligands have two sulfonyl groups, which can be easily deprotonated to bind metal centers due to the stronger chelating ability of $-SO_3^-$ groups to form cyclic coordinated configurations with neighboring $-CO_2^-$ or $-SO_3^-$ groups (Scheme 1).[19,35] The coordination of the $-SO_3^-$ group to metal centers will reduce the proton concentration and the porosity of the resulting MOFs, so that the proton conductivity may be greatly decreased.[28]

Our previous work also demonstrated that the MOF (Me_2NH_2)[Eu(2,2′-**DSBPDC**)(H_2O)] based on a 2,2′-**DSBPDC** ligand showed a relatively low proton conductivity (4.14×10^{-8} S cm^{-1}) at 25 °C and 95% RH owing to the coordination of two deprotonated sulfonyl groups to the metal center (Scheme 2).[33] Therefore, our present strategy for preparing proton conductive MOFs is to design a mono-sulfonated substituted carboxylic ligand: 2-sulfonyl-4,4′-biphenyldicarboxylic acid (**H_3L**) as shown in Scheme 2. We expect that the coordination of the $-SO_3H$ group of **H_3L** to metal ions can be avoided so that the group may be completely free in the form of $-SO_3^-$ or acidic $-SO_3H$. Surprisingly, this kind of seemingly simple ligand is very elusive in the literature and has never been applied for the construction of MOFs and related proton-conducting materials to date.[36] Compared to the disulfonyl-substituted one, the mono-sulfonated ligand with only one $-SO_3H$ group will possess less steric hindrance and the resulting MOFs can host more protic cations such as dimethylammonium or hydronium, due to the larger porosity.[37–39]

In order to demonstrate our conceptual approach, herein we first synthesized the **H_3L** ligand using a Suzuki C–C coupling reaction between 4-iodo-3-sulfobenzoic acid and 4-carboxyphenylboronic acid (Scheme 3). Using the **H_3L** ligand to react with lanthanide salts, a series of three-dimensional (3D) MOFs, $(Me_2NH_2)_2(H_3O)[LnL_2]\cdot 8H_2O$ (Ln = Eu (**1**), Gd (**2**), Tb (**3**)) have been constructed. Single crystal X-ray diffraction analysis revealed that **1–3** all adopted the doubly interpenetrated 3D **dia** topology. Interestingly, due to the presence of a high concentration of dimethylammonium and, hydronium cations and hanging sulfonic acid groups within the 1D rhombic pore,

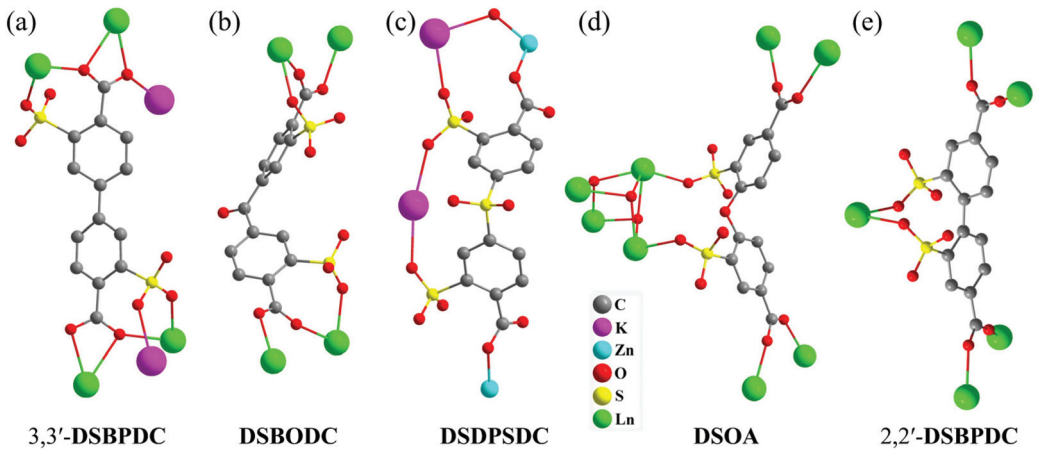

Scheme 1 The coordination modes of some disulfonyl group substituted carboxylic ligands.

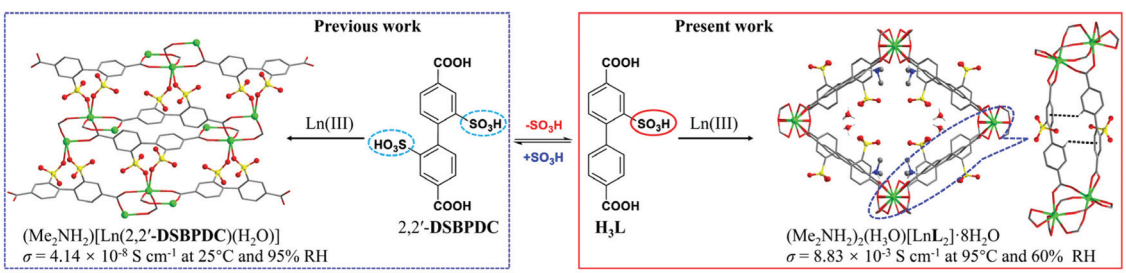

Scheme 2 The comparison of the MOFs built from 2,2′-**DSBPDC** and **H_3L**.

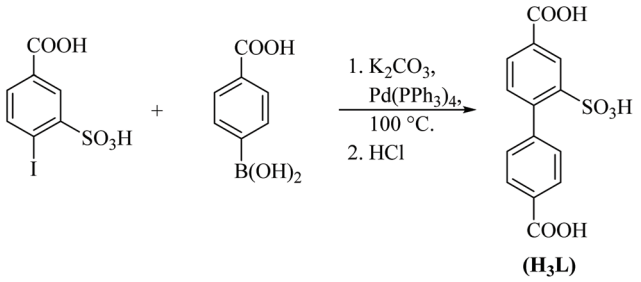

Scheme 3 Synthesis of 2-sulfonyl-4,4′-biphenyldicarboxylic acid (H_3L).

1–3 display a high proton conductivity (8.83×10^{-3} S cm^{-1}) at 95 °C and 60% RH (Scheme 2). More importantly, this ultra-high proton conductivity can be maintained over 72 hours without any significant decrease. This work highlights the fact that mono-sulfonated carboxylic acids are a class of attractive ligands for the construction of proton conductive MOF materials.

2. Experimental

2.1 Materials and methods

All chemical reagents were purchased and used as received. 4-Iodo-3-sulfobenzoic acid was synthesized according to the reference protocols.[33,34] ^{1}H NMR spectra were recorded on a Bruker AM 400 MHz spectrometer in DMSO-d_6 solution, and the chemical shifts are in ppm. FT-IR spectra were recorded on a Nicolet 380 FT-IR instrument (KBr pellets). Powder X-ray diffraction (PXRD) data were collected on a Bruker D8 Advance diffractometer under Cu K_α radiation (λ = 1.5406 Å). C, H, N, and S analyses were conducted using a Thermo Finnigan Flash 1112A elemental analyzer. Thermogravimetric analyses (TGA) were performed on a NETZSCH STA 449C thermal analyzer under a N_2 atmosphere with the heating rate of 5 °C min^{-1}.

2.2 Syntheses of the H_3L ligand and MOFs 1–3

2.2.1 Synthesis of 2-sulfonyl-4,4′-biphenyldicarboxylic acid (H_3L). 4-Iodo-3-sulfobenzoic acid (7.7600 g, 0.0216 mol), 4-carboxyphenylboronic acid (3.4866 g, 0.0216 mol), potassium carbonate (4.9691 g, 0.0360 mol), tetrakis(triphenylphosphine) palladium(0) (830.0 mg, 0.720 mmol), 1,4-dioxane and water (40 mL, 1 : 1) were mixed together in a three-neck flask under N_2. The mixture was heated to 100 °C for 24 hours. After cooling to room temperature (RT), the resulting precipitate was filtered and washed with water (3 × 10 mL). The combined filtrate was concentrated to 20 mL and acidified with hydrochloric acid (36% w/w, 5 mL). The white solid was filtered and washed with water (3 × 10 mL) and acetonitrile (3 × 10 mL) and then dried in a vacuum to give the product **H_3L**. Yield 4.2933 g (61.7%). ^{1}H NMR (400 MHz, DMSO-d_6, δ ppm): 12.95 (2H, COOH), 8.55 (1H, ArH), 7.93 (1H, ArH), 7.88–7.91 (2H, ArH), 7.67 (2H, ArH), 7.28 (1H, ArH). mp >300 °C. FT-IR (KBr, cm^{-1}): 3478(br, m), 3119(m), 1713(vs), 1605(m), 1404(m), 1225(s), 1189(s), 1041(m), 852(w), 623(m). Anal. calcd for $C_{14}H_{10}O_7S$ (%): C 52.17, H 3.13, S 9.95; found: C 52.01, H 3.28, S 9.85.

The **H_3L** ligand is insoluble in common solvents, such as water, methanol, ethanol, acetone, acetonitrile, dichloromethane and chloroform. It is only soluble in *N*,*N*-dimethylformamide (DMF) and dimethyl sulfoxide.

2.2.2 Synthesis of $(Me_2NH_2)_2(H_3O)[EuL_2]\cdot 8H_2O$ (1). A mixture of $Eu(NO_3)_3\cdot 6H_2O$ (8.9 mg, 0.02 mmol), **H_3L** (15.1 mg, 0.04 mmol), dimethylamine hydrochloride ($Me_2NH\cdot HCl$) (20.0 mg, 0.25 mmol), and DMF (4 mL) was heated in a 25 mL stainless-steel reactor lined with Teflon at 150 °C for 48 h and then cooled to RT within 24 h. Colorless block-shaped crystals of **1** were collected by filtration and washed with ethanol (3 × 5 mL). The yield was 81.0% (16.9 mg) based on Eu(III). FT-IR (KBr, cm^{-1}): 3345(br, m), 1585(m), 1408(vs), 1225(m), 1184(m), 1041(m), 630(m). Anal. calcd for $C_{32}H_{49}EuN_2O_{23}S_2$ (%): C 36.75, H 4.72, N 2.68, S 6.13; found: C 36.65, H 4.59, N 2.54, S 6.02.

2.2.3 Synthesis of $(Me_2NH_2)_2(H_3O)[GdL_2]\cdot 8H_2O$ (2). The procedure was the same as that for **1** except for using $Gd(NO_3)_3\cdot 6H_2O$ (9.0 mg, 0.02 mmol) instead of $Eu(NO_3)_3\cdot 6H_2O$. The yield of **2** was 83.4% (17.5 mg) based on Gd(III). FT-IR (KBr, cm^{-1}): 3445(m), 1578(m), 1401(vs), 1225(m), 1190(m), 1041(s), 630(m). Anal. calcd for $C_{32}H_{49}GdN_2O_{23}S_2$ (%): C 36.57, H 4.70, N 2.67, S 6.10; found: C 36.39, H 4.51, N 2.50, S 6.01.

2.2.4 Synthesis of $(Me_2NH_2)_2(H_3O)[TbL_2]\cdot 8H_2O$ (3). The procedure was the same as that for **1** except for using $Tb(NO_3)_3\cdot 6H_2O$ (9.1 mg, 0.02 mmol) instead of $Eu(NO_3)_3\cdot 6H_2O$. The yield of **3** was 80.0% (16.8 mg) based on Tb(III). FT-IR (KBr, cm^{-1}): 3421(m), 1588(m), 1420(vs), 1229(m), 1180(m), 1040(s). Anal. calcd for $C_{32}H_{49}TbN_2O_{23}S_2$ (%): C 36.51, H 4.69, N 2.66, S 6.09; found: C 36.37, H 4.57, N 2.51, S 6.18.

2.3 Single crystal X-ray diffraction analysis

Single-crystal X-ray diffraction data for **1–3** were recorded on a Bruker Apex II CCD with a Mo K_α X-ray source (λ = 0.71073 Å) at RT. These structures were determined *via* direct methods with the SHELXTL-2018 software package.[40] The crystallographic data of **1–3** are presented in Table S1.† The main bond distances and angles are summarized in Table S2.† These data (CCDC 2054977–2054979 for **1–3**,† respectively) are available.

2.4 Proton conductivity measurement

The alternating current (AC) conductivity measurements for **2** were performed on a pressed cuboid-shaped plate (8 × 8 × 0.80 mm) made under a pressure of ~15 MPa. The two faces of the plate were coated with silver paste and then the plates were pressed between parallel square titanium electrodes in specially designed porous quartz cells. The AC impedance data were obtained under different environmental conditions by an ordinary quasi-four-probe method, making use of silver wires and paste with a CHI 660E electrochemical workstation in the frequency range of 1 MHz–0.1 Hz with an input voltage amplitude of 100 mV. The temperature and humidity parameters were controlled using the SW/HS-50A temperature and humidity control chamber. The Zview software was used to determine

the resistance value from the equivalent circuit fit of the first semi-circle.

Proton conductivity was calculated using the following equation:

$$\sigma = \frac{l}{SR} \quad (1)$$

where l and S are the length (cm) and cross-sectional area (cm^2) of the pressed plate respectively, and R, which was extracted from the Nyquist plots, is the bulk resistance of the sample (Ω). Activation energy (E_a) for the conductivity of materials was estimated from the following equation:

$$\sigma T = \sigma_0 \exp\left(-\frac{E_a}{k_B T}\right) \quad (2)$$

where σ is the proton conductivity, σ_0 is the preexponential factor, k_B is the Boltzmann constant, and T is the temperature.

3. Results and discussion

Although the **H_3L** ligand was first mentioned in a US patent in 2012,[36] its spectral characterization, yield and related complexes were not reported. Using a Suzuki C–C coupling reaction between 4-iodo-3-sulfobenzoic acid and 4-carboxyphenylboronic acid (Scheme 3), the **H_3L** ligand was successfully prepared in a good yield and characterized by elemental analysis, FT-IR (Fig. S1†) and ^{1}H NMR (Fig. S2†).

The solvothermal reaction of the **H_3L** ligand with lanthanide salts $Ln(NO_3)_3{\cdot}6H_2O$ (Ln = Eu, Gd, Tb) and $Me_2NH{\cdot}HCl$ in DMF gave the corresponding MOFs **1–3** in high yields. Single-crystal X-ray diffraction analysis shows that all the MOFs **1–3** are isomorphous and crystallize in the same orthorhombic system with a space group of *Pnnn* (Table S1†). Due to the structural similarity of **1–3**, only the structure of **2** is discussed here in detail. The asymmetric unit of **2** contains a Gd(III) cation (the occupancy factor is 0.5), one L^{3-} ligand, one $(Me_2NH_2)^+$ cation, one H_3O^+ cation (the occupancy factor is 0.5), and four highly disordered lattice water molecules (Fig. S4†). The presence of the counterions and guest water molecules has been further confirmed by elemental analysis, FT-IR (Fig. S7†) and TGA measurements (Fig. S13†). The Gd(III) center is coordinated by eight carboxylic O atoms from six different L^{3-} ligands. Among the eight O atoms, four O atoms are from two chelating carboxylic groups, while the others are from four bridging carboxylic groups (Fig. 1d). The GdO_8 unit exhibits a distorted dodecahedral geometry (Fig. 1a). The Gd–O distances (2.311(4)–2.485(4) Å) are comparable to those usually found in the related Gd-MOFs (Table S2†).[41] Each Gd(III) ion is linked to the nearby one through four bridging carboxylic groups to form a $[Gd(-COO)_4Gd]^{2+}$ dimer with a Gd···Gd distance of 4.195(4) Å (Fig. 1d). Each dimer is further joined to four adjacent ones by a pair of L^{3-} ligands in a head to tail connection mode (Fig. 1c), which can be regarded as a double-walled linker (Fig. 1d). Notably, the double-walled linker is further supported by two intermolecular edge-to-face C6–H6···π^v interactions with a distance of 3.943(2) Å and an angle ∠C6–H6···π^v of 134° between the phenyl rings (Fig. 1c and Table S3†). Therefore, by means of the double-walled linkers connecting to the dimers, a stable 3D framework in **2** can be finally formed (Fig. 1e and f). Topologically, if each double-walled linker is simplified as a straight line (Fig. 1c) and each $[Gd(-COO)_4Gd]^{2+}$ dimer is regarded as a 4-connected node (Fig. 1d), the 3D framework of **2** can be simplified as a **dia** net topology (Schläfli symbol of 6^6) as shown in Fig. 1e. The side length of the **dia** net is 15.831(13) Å, whereas the

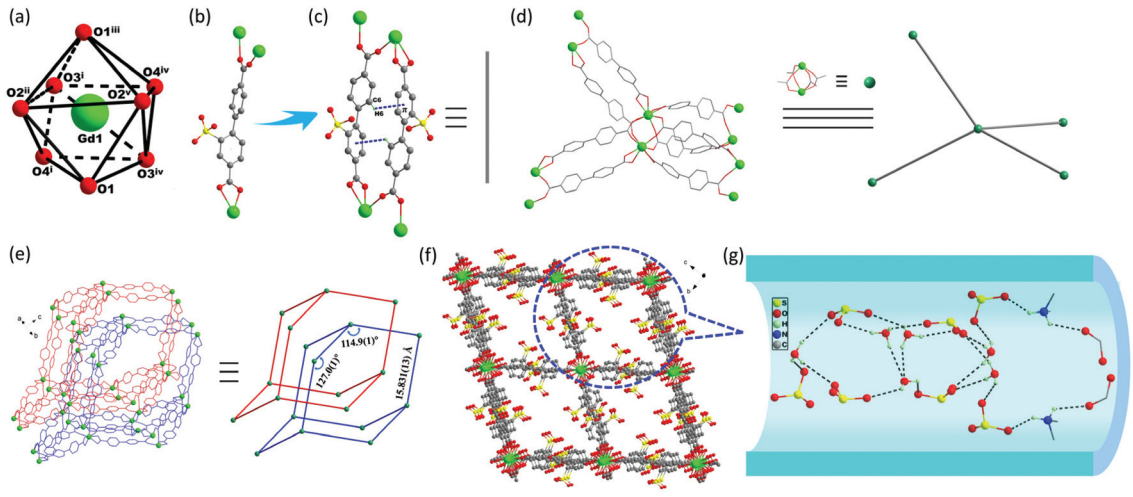

Fig. 1 (a) A distorted dodecahedral geometry of the Gd1 atom. (b) The coordinated modes of L^{3-} ligands. (c) A pair of L^{3-} ligands in a head to tail connection mode supported by two C–H···π interactions. (d) A Gd_2 dimer connected by four double-walled linkers was simplified as a 4-connected node. H atoms and sulfonic groups are omitted for clarity. (e) A doubly interpenetrated 3D **dia** net in **2**. H atoms and sulfonic groups are omitted for clarity. (f) The 3D structure showing 1D rhombic pores with the sulfonic groups along the *a* axis. (g) The H-bonding network consisting of dimethylammonium, hydronium, and sulfonic ions in the 1D pore.

angles are 114.9(1)° and 127.0(1)°, respectively (Fig. 1e), exhibiting an obvious distortion from the tetrahedral angle of 109.5° observed in an ideal diamond. This distortion may be partially resulted from the two-fold interpenetrated structure found in **2** (Fig. 1e). Moreover, despite the double interpenetration, **2** still has a 57.2% solvent accessible volume calculated by PLATON software[42] and possesses 1D rhombic channels along the *a* axis (Fig. 1f). These channels are filled with $(Me_2NH_2)^+$ cations, H_3O^+ cations and lattice water molecules, which form extensive hydrogen-bonded networks with the $-SO_3^-$ groups hanging on the pore walls (Fig. 1g). In addition, there are strong aliphatic C–H···O interactions between the methyl groups of the $(Me_2NH_2)^+$ cation and the carboxylic O atoms in **2** (Table S3,† C15–H15C···O4), which is also manifested by a weak peak at 2800 cm^{-1} in the FT-IR spectrum of **2** (Fig. S7†).[43,44] These abundant hydrogen-bonded networks can be recognized as an important platform for the proton transfer and motion, which will be beneficial for the proton conduction in **2**.

Since the mono-sulfonated **H_3L** ligand is closely related to the disulfonated ligand 2,2′-**DSBPDC**,[33] it would be interesting to compare the structures of the resulting MOFs derived from the same metal ions but differ only in the sulfonate substituents. Interestingly, in the channels of (Me_2NH_2)[Eu(2,2′-**DSBPDC**)(H_2O)],[33] only one dimethylammonium cation per metal unit can be hosted. In contrast, by eliminating one sulfonate group, the present MOF **2** can encapsulate two dimethylammonium cations as the volume of the pores in **2** is enlarged by the removal of one SO_3^- group. Most importantly, eight H_2O molecules and an additional H_3O^+ cation per metal unit have also been included in **2** compared with (Me_2NH_2)[Eu(2,2′-**DSBPDC**)(H_2O)] (only one coordinated water molecule per metal unit).[33] In addition, the two deprotonated sulfonic groups in 2,2′-**DSBPDC** are bound to the same Eu(III) ion in a monodentate mode, forming a nine-membered ring in (Me_2NH_2)[Eu(2,2′-**DSBPDC**)(H_2O)] (Scheme 1e).[33] Consequently, the pores have only 16.7% solvent accessible volume by PLATON analysis.[42] In contrast, the mono sulfonic group of **H_3L** is not involved in the coordination with metal ions, giving 57.2% solvent accessible volume in **2**. Notably, when the same synthesis conditions as those for (Me_2NH_2)[Eu(2,2′-**DSBPDC**)(H_2O)] were used except for replacing 2,2′-**DSBPDC** with **H_3L**, only an unidentified amorphous powder was obtained.

The high concentration of dimethylammonium and, hydronium cations and abundant hydrogen-bonded networks from the hanging sulfonic acid groups within the 1D rhombic pores of **2** encouraged us to investigate the proton conductivity (σ). The Nyquist plots of **2** are shown in Fig. 2. First, the σ value of **2** was evaluated under different RH at RT (Fig. 2a). At 30% RH,

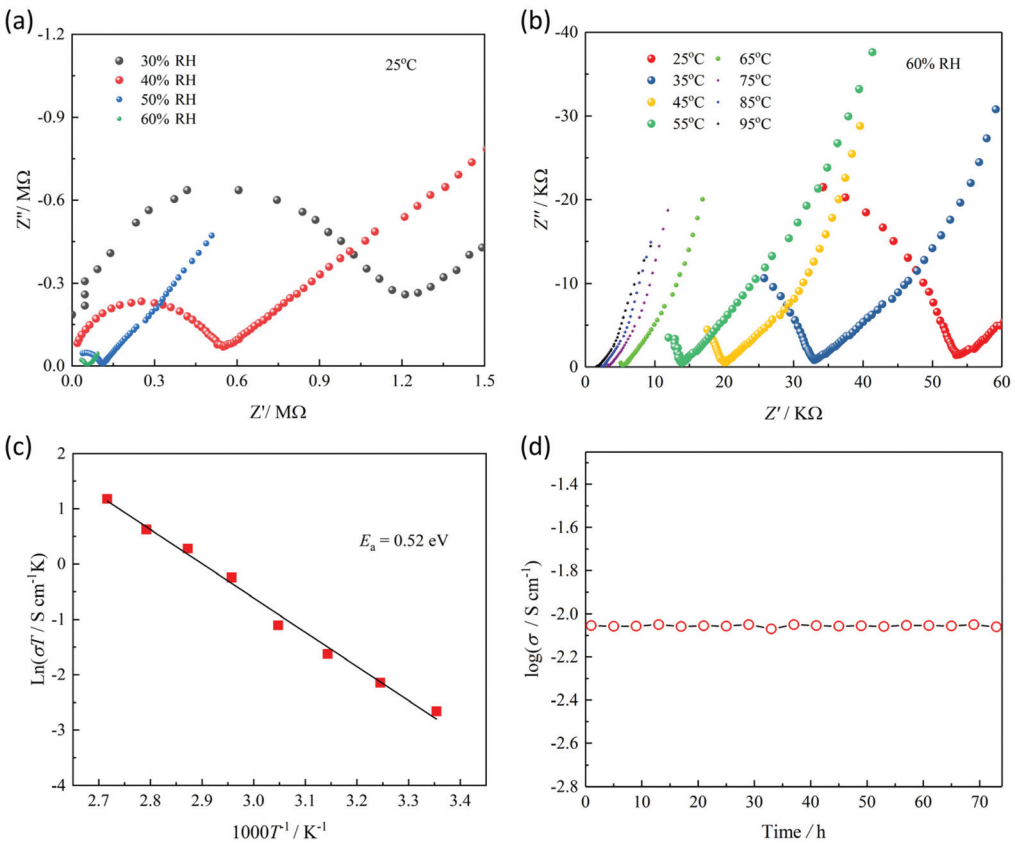

Fig. 2 (a) Impedance spectra of **2** under 30–60% RH at RT. (b) The variable temperature impedance spectra of **2** from 25 to 95 °C at 60% RH. (c) Arrhenius plot. (f). Time-dependent proton conductivity of **2** at 95 °C and 60% RH.

Table 1 Proton conductivities of some representative MOFs at low humidity (<70% RH)

MOFs	σ (S cm^{-1})	Conditions	Ref.
H_2SO_4@MIL-101	6.0×10^{-2}	80 °C/20% RH	45
CF_3SO_3H@MIL-101	5×10^{-2}	25 °C/15% RH	46
IL@MIL-101(SIB-3)	4.4×10^{-2}	50 °C/23% RH	48
VNU-15	2.9×10^{-2}	95 °C/60% RH	17
SPEEK/S-UiO-66@GO-10	1.66×10^{-2}	100 °C/40% RH	49
$(Me_2NH_2)_2(H_3O)[LnL_2]\cdot 8H_2O$	8.83×10^{-3}	95 °C/60% RH	This work
PSM-2	4.6×10^{-3}	80 °C/40% RH	50
$\{(Me_2NH_2)_2(H_2O)_3[Ln_2L_2]\}_n$	1.1×10^{-3}	100 °C/68% RH	51
PCMOF-17	1.17×10^{-3}	25 °C/40% RH	16
PCMOF2(Pz)	3.28×10^{-4}	25 °C/40% RH	52
$[\{(tmen)Pd\}_7(tib)_2(ptp)_2](NO_3)_{14}$	6.56×10^{-4}	23 °C/46% RH	53
[Zn(H5-sip)(4,4′-bpy)]·DMF·2H_2O	3.9×10^{-4}	25 °C/60% RH	54
$[Zn(H_2O)(H5\text{-}sip)(bpel)_{0.5}]\cdot DMF$	3.4×10^{-8}	25 °C/60% RH	54
$[Zn_3(5\text{-}sip)_2(H5\text{-}sip)(4,4'\text{-}bpy)]\cdot DMF\cdot 2DMA$	8.7×10^{-5}	25 °C/60% RH	54
$\{[Co_3(m\text{ClPhIDC})_2(H_2O)_6]\cdot 2H_2O\}_n$	8.69×10^{-5}	100 °C/68% RH	55
$\{R_3N(CH_2CO_2H)\}[MCr(ox)_3]\cdot nH_2O$	8×10^{-5}	25 °C/60% RH	56
NH_2-MIL-53	3×10^{-5}	80 °C/26% RH	57

the σ value of **2** was 1.06×10^{-5} S cm^{-1}, while at 60% RH the value increased to 2.35×10^{-4} S cm^{-1} (Table S4†). However, the effective data points failed to be taken because the samples of **2** cannot be equilibrated above 60% RH. Thus, the variable temperature conductivity of **2** was measured from 35 to 95 °C at 60% RH for the same sample. At 60% RH, the σ value (3.80×10^{-4} S cm^{-1}) of **2** at 35 °C increased rapidly to 8.83×10^{-3} S cm^{-1} at 95 °C (Fig. 2b and Table S4†), making **2** a super proton conductive MOF material under low humidity conditions (<70% RH) (Table 1). The σ value of **2** at 95 °C and 60% RH is only slightly lower than those reported for two strong acid directly doped MOFs, H_2SO_4@MIL-101 (6.0×10^{-2} S cm^{-1})[45] and CF_3SO_3H@MIL-101 (5×10^{-2} S cm^{-1}) (Table 1).[46] The high proton conductivity of **2** under such low humidity conditions may be attributed to the incorporation of hydrophilic sulfonic groups for enhanced binding capacity to the water molecules that are encapsulated inside the MOF channels. Moreover, the high proton conductivity of **2** can be maintained over 72 hours without any significant decrease (Fig. 2d). The activation energy (E_a) of **2** was calculated from the Arrhenius plot (Fig. 2c) to be 0.52 eV, suggesting a conventional vehicle mechanism.[47]

At RT, the σ value (2.35×10^{-4} S cm^{-1}) of **2** under low humidity conditions (60% RH) is much higher than that (4.14×10^{-8} S cm^{-1}) of the MOF (Me_2NH_2)[Eu(2,2′-**DSBPDC**)(H_2O)] at high humidity (95% RH).[33] At an elevated temperature, the σ value (8.83×10^{-3} S cm^{-1} at 95 °C and 60% RH) of **2** is also higher than those found for the disulfonyl-based MOFs at a high RH, **JXNU-2** with 3,3′-**DSBPDC** (1.11×10^{-3} S cm^{-1} at 80 °C and 98% RH),[27] $\{(H_3O)[Ln(\textbf{DSBODC})(H_2O)_2]\}_n$ (6.57×10^{-4} S cm^{-1} at 85 °C and 95% RH),[28] $[K_2Zn(\textbf{DSDPSDC})(H_2O)_4]_n$, ($1.57 \times 10^{-4}$ S cm^{-1} at 85 °C and 95% RH),[29] and $\{[Tb_4(OH)_4(\textbf{DSOA})_2(H_2O)_8]\cdot 8H_2O\}_n$, ($1.66 \times 10^{-4}$ S cm^{-1} at 100 °C and 98% RH).[31] The proton conductivity study of **2** once again confirms the importance of the hanging sulfonic acid groups in the pores of the MOFs in the formation of the proton-mobilizing pathway. By analyzing the structure of **2** and also examining the species encapsulated inside the channels, it is reasonable to assume that the high proton conductivity of **2** at low RH is due to the strong H-bond interactions between the sulfonic groups, the dimethylammonium and hydronium cations. The structural integrity of **2** was further confirmed by the PXRD analysis of the samples before and after the measurements, which show the same patterns (Fig. S10†). It is to note that, unfortunately, MOF **2** cannot maintain the porosity after three days of water immersion (Fig. S11†). The reduced stability of **2** in aqueous media compared to the MOFs from disulfonated ligands is probably due to the enhanced acidity of the MOF caused by the presence of uncoordinated SO_3^- groups that are more reactive upon water immersion. Similar phenomena have been observed previously.[16] Further studies to improve the water stability are in progress and will be reported in due course.

4. Conclusion

In conclusion, we have successfully developed a concept for porosity regulation of MOFs through rational ligand design. By applying asymmetric, mono-sulfonated 2-sulfonyl-4,4′-biphenyldicarboxylic acid as a novel ligand, a series of 3D MOFs containing hanging sulfonic groups have been synthesized and characterized by X-ray crystallography. Due to the elimination of one sulfonate group, coordination of the sulfonate group to metal ions can be avoided and the resulting MOFs have increased porosity and can encapsulate more protic ions. Consequently, an increased proton conductivity (up to 8.83×10^{-3} S cm^{-1} at 95 °C and 60% RH) has been achieved. Furthermore, this high proton conductivity can be maintained over 72 hours without any significant decrease. We believe that this study will unlock an enormous opportunity in ligand design, especially in the area of asymmetric carboxylic acid based ligands and related MOFs. It is to expect that the strat-

egy of regulating the porosity of MOFs by ligand design will be extended in other areas.

Conflicts of interest

There are no conflicts to declare.

Acknowledgements

This work was supported by the National Natural Science Foundation of China (No. 21476115) and the Natural Science Foundation of Jiangsu Province (No. BK20181374). S. Z. thanks the Postgraduate Research & Practice Innovation Program of Jiangsu Province (KYCX20_1027) and the Cultivation Program for the Excellent Doctoral Dissertation of Nanjing Tech University (2020-03) for financial support.

References

1 M. Pan, C. Pan, C. Li and J. Zhao, A review of membranes in proton exchange membrane fuel cells: Transport phenomena, performance and durability, *Renewable Sustainable Energy Rev.*, 2021, **141**, 110771.
2 X. Meng, H. N. Wang, S. Y. Song and H. J. Zhang, Proton-conducting crystalline porous materials, *Chem. Soc. Rev.*, 2017, **46**, 464–480.
3 D.-W. Lim and H. Kitagawa, Proton transport in metal-organic frameworks, *Chem. Rev.*, 2020, **120**, 8416–8467.
4 D.-W. Lim, M. Sadakiyo and H. Kitagawa, Proton transfer in hydrogen-bonded degenerate systems of water and ammonia in metal-organic frameworks, *Chem. Sci.*, 2019, **10**, 16–33.
5 S. Chand, S. M. Elahi, A. Pal and M. C. Das, Metal-organic frameworks and other crystalline materials for ultrahigh superprotonic conductivities of 10^{-2} S cm^{-1} or higher, *Chem. – Eur. J.*, 2019, **25**, 6259–6269.
6 S. C. Pal and M. C. Das, Superprotonic conductivity of MOFs and other crystalline platforms beyond 10^{-1} S cm^{-1}, *Adv. Funct. Mater.*, 2021, **31**, 2101584.
7 M. K. Sarango-Ramírez, J. Park, J. Kim, Y. Yoshida, D.-W. Lim and H. Kitagawa, Void space versus surface functionalization for proton conduction in metal-organic frameworks, *Angew. Chem., Int. Ed.*, 2021, **60**, 20173–20177.
8 Q. Li, R. He, J. O. Jensen and N. J. Bjerrum, Approaches and recent development of polymer electrolyte membranes for fuel cells operating above 100 °C, *Chem. Mater.*, 2003, **15**, 4896–4915.
9 Y. Chen, M. Thorn, S. Christensen, C. Versek, A. Poe, R. C. Hayward, M. T. Tuominen and S. Thayumanavan, Enhancement of anhydrous proton transport by supramolecular nanochannels in comb polymers, *Nat. Chem.*, 2010, **2**, 503–508.
10 Z. Li, G. He, B. Zhang, Y. Cao, H. Wu, Z. Jiang and T. Zhou, Enhanced proton conductivity of Nafion hybrid membrane under different humidities by incorporating metal-organic frameworks with high phytic acid loading, *ACS Appl. Mater. Interfaces*, 2014, **6**, 9799–9807.
11 V. G. Ponomareva, A. M. Cheplakova, K. A. Kovalenko and V. P. Fedin, Exceptionally stable H_3PO_4@MIL-100 system: A correlation between proton conduction and water adsorption properties, *J. Phys. Chem. C*, 2020, **124**, 23143–23149.
12 S. Liu, Z. Yue and Y. Liu, Incorporation of imidazole within the metal-organic framework UiO-67 for enhanced anhydrous proton conductivity, *Dalton Trans.*, 2015, **44**, 12976–12980.
13 X. L. Sun, W. H. Deng, H. Chen, H. L. Han, J. M. Taylor, C. Q. Wan and G. Xu, A metal-organic framework impregnated with a binary ionic liquid for safe proton conduction above 100 °C, *Chem. – Eur. J.*, 2017, **23**, 1248–1252.
14 W. J. Liu, L. Z. Dong, R. H. Li, Y. J. Chen, S. N. Sun, S. L. Li and Y. Q. Lan, Different protonic species affecting proton conductivity in hollow spherelike polyoxometalates, *ACS Appl. Mater. Interfaces*, 2019, **11**, 7030–7036.
15 P. Chen, S. Liu, Z. Bai and Y. Liu, Enhanced ionic conductivity of ionic liquid confined in UiO-67 membrane at low humidity, *Microporous Mesoporous Mater.*, 2020, **305**, 110369.
16 B. Joarder, J. B. Lin, Z. Romero and G. K. H. Shimizu, Single crystal proton conduction study of a metal organic framework of modest water stability, *J. Am. Chem. Soc.*, 2017, **139**, 7176–7179.
17 T. N. Tu, N. Q. Phan, T. T. Vu, H. L. Nguyen, K. E. Cordova and H. Furukawa, High proton conductivity at low relative humidity in an anionic Fe-based metal-organic framework, *J. Mater. Chem. A*, 2016, **4**, 3638–3641.
18 J. Jiang and O. M. Yaghi, Brønsted acidity in metal-organic frameworks, *Chem. Rev.*, 2015, **115**, 6966–6997.
19 R.-L. Liu, D.-Y. Wang, J.-R. Shi and G. Li, Proton conductive metal sulfonate frameworks, *Coord. Chem. Rev.*, 2021, **431**, 213747.
20 S. Mukhopadhyay, J. Debgupta, C. Singh, R. Sarkar, O. Basu and S. K. Das, Designing UiO-66-based superprotonic conductor with the highest metal-organic framework based proton conductivity, *ACS Appl. Mater. Interfaces*, 2019, **11**, 13423–13432.
21 S. Devautour-Vinot, E. S. Sanil, A. Geneste, V. Ortiz, P. G. Yot, J.-S. Chang and G. Maurin, Guest-assisted proton conduction in the sulfonic mesoporous MIL-101 MOF, *Chem. – Asian J.*, 2019, **14**, 3561–3565.
22 W. J. Phang, H. Jo, W. R. Lee, J. H. Song, K. Yoo, B. Kim and C. S. Hong, Superprotonic conductivity of a UiO-66 framework functionalized with sulfonic acid groups by facile postsynthetic oxidation, *Angew. Chem., Int. Ed.*, 2015, **54**, 5142–5146.
23 X.-M. Li, L.-Z. Dong, S.-L. Li, G. Xu, J. Liu, F.-M. Zhang, L.-S. Lu and Y.-Q. Lan, Synergistic conductivity effect in a proton sources-coupled metal-organic framework, *ACS Energy Lett.*, 2017, **2**, 2313–2318.
24 Y. Wang, G. Ye, H. Chen, X. Hu, Z. Niu and S. Ma, Functionalized metal-organic framework as a new platform

for efficient and selective removal of cadmium(II) from aqueous solution, *J. Mater. Chem. A*, 2015, **3**, 15292–15298.
25 J. Jiang, F. Gandara, Y.-B. Zhang, K. Na, O. M. Yaghi and W. G. Klemperer, Superacidity in sulfated metal-organic framework-808, *J. Am. Chem. Soc.*, 2014, **136**, 12844–12847.
26 L. Zhao, R.-R. Zhu, S. Wang, L. He, L. Du and Q.-H. Zhao, Multiple strategies to fabricate a highly stable 2D $Cu^{II}Cu^{I}$-organic framework with high proton conductivity, *Inorg. Chem.*, 2021, **21**, 16474–16483.
27 L. J. Zhou, W. H. Deng, Y. L. Wang, G. Xu, S. G. Yin and Q. Y. Liu, Lanthanide-potassium biphenyl-3,3′-disulfonyl-4,4′-dicarboxylate frameworks: gas sorption, proton conductivity, and luminescent sensing of metal ions, *Inorg. Chem.*, 2016, **55**, 6271–6277.
28 W. W. Zhang, Y. L. Wang, Q. Liu and Q. Y. Liu, Lanthanide-benzophenone-3,3′-disulfonyl-4,4′-dicarboxylate frameworks: Temperature and 1-hydroxypyren luminescence sensing and proton conduction, *Inorg. Chem.*, 2018, **57**, 7805–7814.
29 X.-Y. Zeng, Y.-L. Wang, Z.-T. Lin and Q.-Y. Liu, Proton-conductive coordination polymers based on diphenylsulfone-3,3′-disulfo-4,4′-dicarboxylate with well-defined hydrogen bonding networks, *Inorg. Chem.*, 2020, **59**, 12314–12321.
30 X.-Y. Dong, R. Wang, J.-B. Li, S.-Q. Zang, H.-W. Hou and T. C. W. Mak, A tetranuclear $Cu_4(\mu_3\text{-}OH)_2$-based metal-organic framework (MOF) with sulfonate-carboxylate ligands for proton conduction, *Chem. Commun.*, 2013, **49**, 10590–10592.
31 X.-Y. Dong, R. Wang, J.-Z. Wang, S.-Q. Zang and T. C. W. Mak, Highly selective Fe^{3+} sensing and proton conduction in a water-stable sulfonate-carboxylate Tb-organic-framework, *J. Mater. Chem. A*, 2015, **3**, 641–647.
32 S. P. Bera, A. Mondal, S. Roy, B. Dey, A. Santra and S. Konar, 3D isomorphous lanthanide coordination polymers displaying magnetic refrigeration, slow magnetic relaxation and tunable proton conduction, *Dalton Trans.*, 2018, **47**, 15405–15415.
33 J. Zhao, X. He, Y. Zhang, J. Zhu, X. Shen and D. Zhu, Highly water stable lanthanide metal-organic frameworks constructed from 2,2′-disulfonyl-4,4′-biphenyldicarboxylic acid: Syntheses, structures, and properties, *Cryst. Growth Des.*, 2017, **17**, 5524–5532.
34 S. Zhang, S. Gao, X. Wang, X. He, J. Zhao and D. Zhu, Two topologically different 3D Cu^{II} metal-organic frameworks assembled from the same ligands: control of reaction conditions, *Acta Crystallogr., Sect. B: Struct. Sci., Cryst. Eng. Mater.*, 2019, **75**, 1060–1068.
35 M. Furtmair, J. Timm and R. Marschall, Sulfonation of porous materials and their proton conductivity, *Microporous Mesoporous Mater.*, 2021, **312**, 110745.
36 P. I. Lazarev, *US Patent* US20120099052A1, 2012.
37 B. Joarder, J.-B. Lin, Z. Romero and G. K. H. Shimizu, Single crystal proton conduction study of a metal organic framework of modest water stability, *J. Am. Chem. Soc.*, 2017, **139**, 7176–7179.
38 T.-T. Guo, D.-M. Cheng, J. Yang, X. Xu and J.-F. Ma, Calix[4]resorcinarene-based $[Co_{16}]$ coordination cages mediated by isomorphous auxiliary ligands for enhanced proton conduction, *Chem. Commun.*, 2019, **55**, 6277–6280.
39 F. Yang, G. Xu, Y. Dou, B. Wang, H. Zhang, H. Wu, W. Zhou, J.-R. Li and B. Chen, A flexible metal-organic framework with a high density of sulfonic acid sites for proton conduction, *Nat. Energy*, 2017, **2**, 877–883.
40 G. Sheldrick, Crystal structure refinement with SHELXL, *Acta Crystallogr., Sect. C: Struct. Chem.*, 2015, **71**, 3–8.
41 X. Wang, J. Zhao, Y. Zhao, H. Xu, X. Shen, D. R. Zhu and S. Jing, Three sra topological lanthanide-organic frameworks built from 2,2′-dimethoxy-4,4′-biphenyldicarboxylic acid, *Dalton Trans.*, 2015, **44**, 9281–9288.
42 A. Spek, Single-crystal structure validation with the program PLATON, *J. Appl. Crystallogr.*, 2003, **36**, 7–13.
43 A. Elaiwi, P. B. Hitchcock, K. R. Seddon, N. Srinivasan, Y.-M. Tan, T. Welton and J. A. Zora, Hydrogen bonding in imidazolium salts and its implications for ambient-temperature halogenoaluminate(III) ionic liquids, *J. Chem. Soc., Dalton Trans.*, 1995, **21**, 3467–3472.
44 Z. Fei, D. Zhao, T. J. Geldbach, R. Scopelliti and P. J. Dyson, Brønsted acidic ionic liquids and their zwitterions: synthesis, characterization and pKa determination, *Chem. – Eur. J.*, 2004, **10**, 4886–4893.
45 V. G. Ponomareva, K. A. Kovalenko, A. P. Chupakhin, D. N. Dybtsev, E. S. Shutova and V. P. Fedin, Imparting high proton conductivity to a metal-organic framework material by controlled acid impregnation, *J. Am. Chem. Soc.*, 2012, **134**, 15640–15643.
46 D. N. Dybtsev, V. G. Ponomareva, S. B. Aliev, A. P. Chupakhin, M. R. Gallyamov, N. K. Moroz, B. A. Kolesov, K. A. Kovalenko, E. S. Shutova and V. P. Fedin, High proton conductivity and spectroscopic investigations of metal-organic framework materials impregnated by strong acids, *ACS Appl. Mater. Interfaces*, 2014, **6**, 5161–5167.
47 X. Wang, T. Qin, S.-S. Bao, Y.-C. Zhang, X. Shen, L.-M. Zheng and D. Zhu, Facile synthesis of a water stable 3D Eu-MOF showing high proton conductivity and its application as a sensitive luminescent sensor for Cu^{2+} ions, *J. Mater. Chem. A*, 2016, **4**, 16484–16489.
48 J. Du, G. Yu, H. Lin, P. Jie, F. Zhang, F. Qu, C. Wen, L. Feng and X. Liang, Enhanced proton conductivity of metal organic framework at low humidity by improvement in water retention, *J. Colloid Interface Sci.*, 2020, **573**, 360–369.
49 H. Sun, B. Tang and P. Wu, Rational design of S-UiO-66@GO hybrid nanosheets for proton exchange membranes with significantly enhanced transport performance, *ACS Appl. Mater. Interfaces*, 2017, **9**, 26077–26087.
50 S. Mukhopadhyay, J. Debgupta, C. Singh, R. Sarkar, O. Basu and S. K. Das, Designing UiO-66-based superprotonic conductor with the highest metal-organic framework based proton conductivity, *ACS Appl. Mater. Interfaces*, 2019, **11**, 13423–13432.

51 R. Wang, X.-Y. Dong, H. Xu, R.-B. Pei, M.-L. Ma, S.-Q. Zang, H.-W. Hou and T. C. W. Mak, A super water-stable europium-organic framework: Guests inducing low-humidity proton conduction and sensing of metal ions, *Chem. Commun.*, 2014, **50**, 9153–9156.
52 S. Kim, B. Joarder, J. A. Hurd, J. Zhang, K. W. Dawson, B. S. Gelfand, N. E. Wong and G. K. H. Shimizu, Achieving superprotonic conduction in metal-organic frameworks through iterative design advances, *J. Am. Chem. Soc.*, 2018, **140**, 1077–1082.
53 D. Samanta and P. S. Mukherjee, Structural diversity in multinuclear Pd(II) assemblies that show low-humidity proton conduction, *Chem. – Eur. J.*, 2014, **20**, 5649–5656.
54 P. Ramaswamy, R. Matsuda, W. Kosaka, G. Akiyama, H. Joon Jeon and S. Kitagawa, Highly proton conductive nanoporous coordination polymers with sulfonic acid groups on the pore surface, *Chem. Commun.*, 2014, **50**, 1144–1146.
55 X. Liang, B. Li, M. Wang, J. Wang, R. Liu and G. Li, Effective approach to promoting the proton conductivity of metal-organic frameworks by exposure to aqua-ammonia vapor, *ACS Appl. Mater. Interfaces*, 2017, **9**, 25082–25086.
56 M. Sadakiyo, H. Ōkawa, A. Shigematsu, M. Ohba, T. Yamada and H. Kitagawa, Promotion of low-humidity proton conduction by controlling hydrophilicity in layered metal-organic frameworks, *J. Am. Chem. Soc.*, 2012, **134**, 5472–5475.
57 J. Liu, X. Zou, C. Liu, K. Cai, N. Zhao, W. Zheng and G. Zhu, Ionothermal synthesis and proton-conductive properties of NH_2-MIL-53 MOF nanomaterials, *CrystEngComm*, 2016, **18**, 525–528.